Available online at www.sciencedirect.com

ScienceDirect

Procedia Engineering 64 (2013) 1384 – 1394

Procedia Engineering

www.elsevier.com/locate/procedia

International Conference On DESIGN AND MANUFACTURING, IConDM 2013

Heterogeneity of microstructure and mechanical properties of friction stir welded joints of Al-Zn-Mg alloy AA7039

Chaitanya Sharma [a,b]*, Dheerendra Kumar Dwivedi [c], Pradeep Kumar [d]

[a, c, d] Mechanical and Industrial Engineering Department, Indian Institute of Technology, Roorkee, Uttarkhand, India-247667
[b] Mechanical Engineering Department, Ideal Institute of Technology, Ghaziabad, Uttar Pradesh, India-201301

Abstract

Al-Zn-Mg aluminium alloy AA7039 was friction stir welded in order to investigate the influence of structural heterogeneity on mechanical properties of welded joints. Quality and mechanical properties of the developed weld joints were assessed by conducting bend, tensile and microhardness tests. Optical and scanning electron microscopy was used to analyze the microstructure and fracture surfaces respectively. It was found that joints were heterogeneous as different layers of joint exhibited significant heterogeneity in respect of microstructure and mechanical properties. Weld nugget grain size was found to decrease from top to bottom. Top layer of joint was strongest while middle layer was weakest. Weight % of Zn and Mg decreased from top to bottom layer of the joint. Mode of fracture was also found to be different for different layers of joint.

Keywords:
Friction stir welding; heterogeneity; microstructure; mechanical properties, fracture.

1. Introduction

Friction stir welding (FSW) is an autogeneous solid state joining process, which eliminates problems related with fusion welding of aluminium alloys owing to its nature (joining in solid state) beside offering better joints properties than fusion weld joints [1, 2]. In general, during FSW deformational and frictional heat is supplied from top side of the plates and combination of severe thermo mechanical stresses softened the material beneath the tool shoulder. Further, simultaneous tool rotation and traverse moves softened material from advancing side (AS) to the

* Corresponding author. Tel.: +91-1332-285826; fax: +91-1332 -285665.
E-mail address: chaitanya.sharmaji@gmail.com

doi:10.1016/j.proeng.2013.09.220

other side to form a joint due to dual action of extrusion and forging [3, 4]. Distribution of thermo mechanical stresses is not uniform along transverse and longitudinal cross section of the weld as maximum temperature has reported to vary from top to bottom surface and from central weld nugget zone (WNZ) to outermost heat affected zone (HAZ) [5-10]. Moreover, different zones of FSW joints displayed heterogeneity in microstructure and mechanical properties [11-15].

Literature review [1-15] revealed that information on structural heterogeneity and its influence on mechanical properties is scare [13-15] and needs further investigation. Therefore, present study aims to investigate the influence of structural heterogeneity on mechanical properties of friction stir welded joints of AA7039.

2. Material and methods

Chemical composition and mechanical properties of base metal AA7039-T6, of 5 mm thick extruded plates are given in Tables 1.

Table 1, Chemical composition and mechanical properties of base metal

Chemical composition (wt%)							Mechanical properties			
Al	Zn	Mg	Mn	Fe	Si	Cu	Ultimate tensile strength (MPa)	Yield strength (MPa)	Elongation (%)	Microhardnes (Hv)
Bal.	4.69	2.37	0.68	0.69	0.31	0.05	414	328	15.1	135

Friction stir welding of AA7039 plates of size 300 X 50 mm^2 was performed parallel to plate extrusion direction using vertical milling machine (HMT India, 7 K.W. and 635 rpm). These plates were held firmly in butt joint position using specially designed fixture. A single pass welding procedure was used to fabricate the joints from one side. The truncated conical tool made of die steel was used for producing FSW joints using tool geometry and welding parameters enlisted in Table 2. These parameters were selected based on earlier work of present authors [16] on the effect of FSW process parameters on microstructure and mechanical properties of friction stir welded joints of AA7039 aluminum alloy. Tool pin has anticlockwise threads of 1mm pitch to facilitate the downward flow of plasticized material beneath the shoulder. A constant tool tilt of 2.5^0 from the vertical axis was also used in order to facilitate the consolidation of plasticized material.

Table 2, Tool dimension and welding parameters used for FSW

Tool dimensions				Welding parameters		
Shoulder diameter (mm)	Pin diameter (mm) Top	Bottom	Pin length (mm)	Welding speed (mm/min)	Rotary speed (rpm)	Tool tilt (degrees)
16	6	4	4.7	75	635	2.5

Weld joints were inspected visually for voids, cracks, and other surface defects if any. Thereafter, weld joints were subjected to three point face and root bend tests to reveal the presence of subsurface defects. FSW joints passed the face and root bend tests successfully and no crack was observed on external surface subjected to bending as shown in the fig. 1. Scheme of obtaining tensile specimen from different thickness position of joint is shown in fig. 2. It is important to note that each time a fresh part of joint was used to obtain flat tensile specimens of 1.5 mm thickness from a particular location by machining i.e. top, middle and bottom region of the joints according to ASTM E8M guidelines [17].

Computerized universal testing machine (H25K-S, Hounsfield) was used for conducting tensile and bend tests at a cross head speed of 1 mm/min. The 0.2% offset yield strength, ultimate tensile strength, strain and % elongation upto fracture were recorded. A Vickers microhardness tester (VHM-002V Walter UHL, Germany) was employed for measuring the microhardness across the joint with a load of 1 N and 30 seconds dwell time.

FSW joints were polished and etched in Keller's reagent (2ml nitric acid, 4ml hydrofluoric acid, and 94 ml water) for 90s for macro and microstructural observation using a light optical microscope (Leica, Germany) and field emission scanning electron microscope (FE-SEM) (FEI-Quanta 200®). The fracture surfaces of the tensile tested specimens were investigated by FE-SEM to study the mode of fracture. An electron probe microscopic analyzer (Cameca SX100) was used to determine the weight percentage of zinc and magnesium across the weld joints in transverse direction at different thickness location (top, middle and bottom) of FSW joint. Image analysis of weld micrographs was done using Image J 1.37v, image analyzing software to determine average size of α aluminium grains present in different zones of friction stir welded joints and base metal.

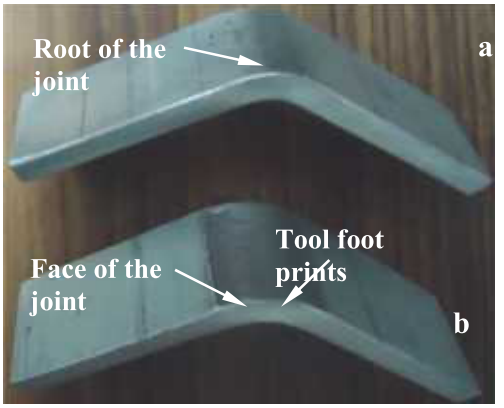

Fig. 1. Friction stir weld joints after (a) root bend , (b) face bend test

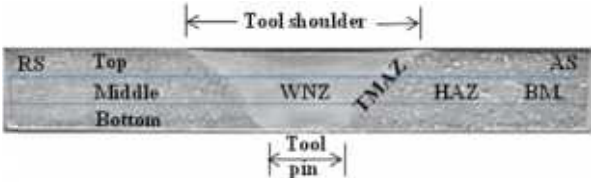

Fig. 2. Macrograph showing the schematic of obtaining tensile specimen from different region of FSW joint

3. Results

3.1 Microstructure

Friction stir welding radically transformed the initial microstructure of the base metal as evident from the macrograph shown in fig. 2 and resulted in the formation of weld nugget zone (WNZ), thermo mechanically affected zone (TMAZ), and heat affected zone (HAZ) in the base metal which are characteristic to friction stir welding process. WNZ of inverted trapezoidal shape had length at top, middle and bottom of 16.6, 8.5 and 4.2 mm respectively (Fig. 2).

The backscattered micrographs of the WNZs, TMAZs and HAZs of different layers of FSW joints are shown in fig. 3, 4 and 5 respectively. WNZ (Fig. 3. a-c) showed fully recrystallized finer grain structure (2.8 to 5.3 times smaller) than base metal (44.3 µm). Size of α aluminium grains was found to decrease from top to bottom layer of the WNZ (Refer table 3).

Table 3, Variation of α Al grain size, microhardness and tensile properties of FSW joints

Joint condition	Size of α Al Grains (µm)			Microhardness (Hv)				Tensile Properties		
	WNZ	TMAZ	HAZ	WNZ	HAZ	Maxima	Minima	Tensile strength (MPa)	Yield strength (MPa)	Elongation (%)
Base metal		44.3				135		414	328	15.1
Top layer	15.5	55.3	90.8	127.8	114.6	146	106	385.4	341.5	15.3
Middle layer	13.1	39.7	75.7	120.6	117.2	142	102	266.1	188.7	12.7
Bottom layer	8.5	26.2	66.7	124.1	119.8	140	108	349.5	265.2	6.7

Few randomly distributed second phase strengthening precipitates $MgZn_2$ can be seen in WNZ than the base metal (Fig. 5. d). These $MgZn_2$ particles appeared as black pits and bright particles (Fig.3. b) in the micrographs as identified by EDAX and EPMA analysis.

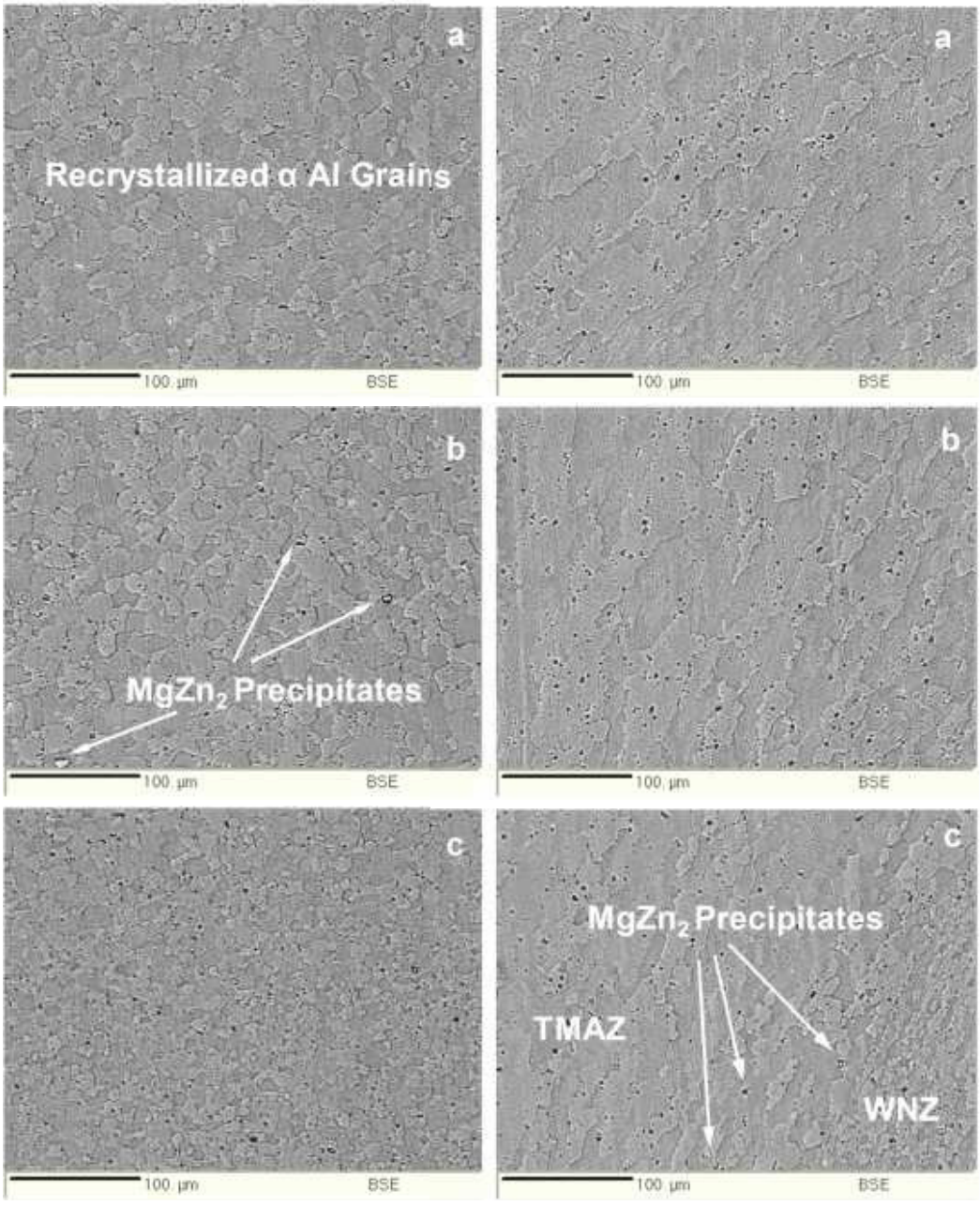

This can be attributed to a) fracture and distribution of $MgZn_2$ particles in WNZ by stirring action of rotating and traversing tool and b) dissolution of these particles in α aluminium matrix as temperature rise is reported to be greater than solutionizing temperature [2]. Moreover, the WNZ of bottom layer exhibited somewhat more

population of second phase strengthening precipitates than top and middle layer of the joint.

TMAZ adjacent to WNZ exhibited elongated non recrystallized grains. The average width of α aluminium grains in TMAZ decreased to 26.2 μm at bottom from 55.3 μm at the top layer of the weld. WNZ-TMAZ interface was sharp and more distinct on AS than retreating side (RS) due to the fact that higher plastic strains and shear flow stresses are experienced by metal in narrow band on AS than RS arising from differences in relative velocity of tool with respect to workpiece in two sides [12].

Grain structure of HAZ was similar to base metal except that α aluminium grains in HAZ were significantly coarsened about 2.1 times than the base metal because of dissolution of fine strengthening precipitate (Fig. 5 a-c). The extent of coarsening was more (2.1 times) at the top layer than the (1.5 times) bottom layer of the weld joint. Moreover, the extent of dissolution of $MgZn_2$ precipitates was found decreasing from top to bottom layer of the joint which was indirectly confirmed by the presence of large size black pits in more numbers.

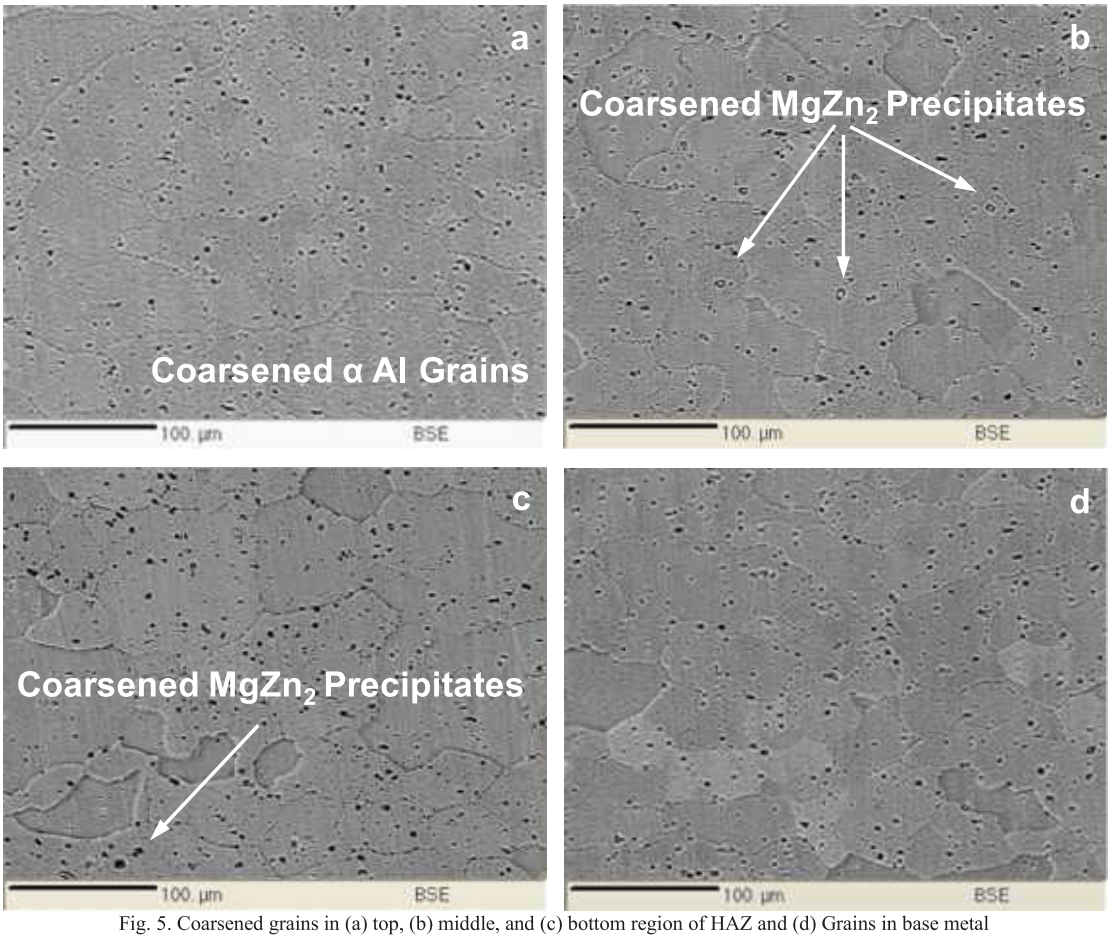

Fig. 5. Coarsened grains in (a) top, (b) middle, and (c) bottom region of HAZ and (d) Grains in base metal

3.2 Microhardness

Microhardness profiles of transverse section of top, middle and bottom layers of FSW joints are shown in fig. 6. Hardness minima were recorded in HAZ on AS while maxima were found on RS of the joints irrespective of weld thickness. Microhardness results are not consistent with α aluminium grain size in WNZ as the same is also greatly affected by the distribution of strengthening precipitates (size, shape and volume) in case of precipitation

hardening aluminium alloys [18] and do not satisfy Hall-Patch relation while reverse trend was observed for HAZ. It was found that microhardness profiles were asymmetric and vary significantly through the thickness of joint (Refer table 3). Top layer exhibited higher microhardness than middle and bottom layer in WNZ. Microhardness of HAZ was found to increase from top to bottom layer of the joint.

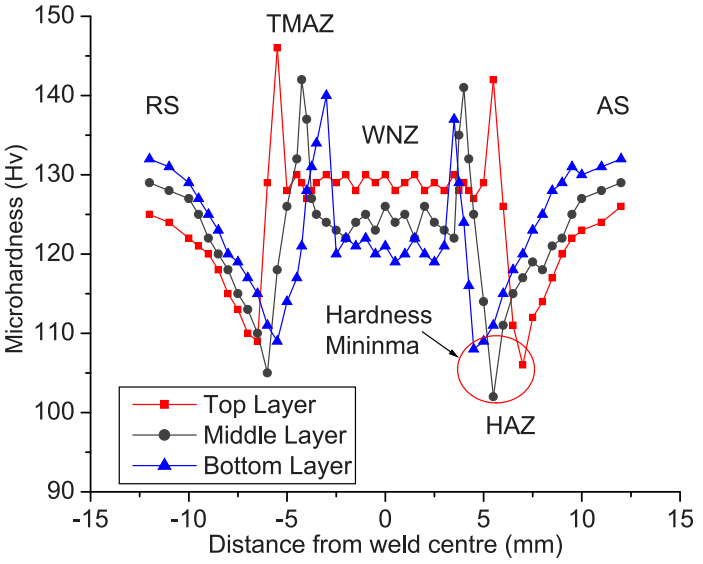

Fig. 6. Microhardness distribution across different layers of FSW joints

EPMA line scans were performed (as shown in fig. 7) across the transverse cross section of the FSW joint in order to show the variation of the Zn and Mg in different zones as well as along the thickness of the joint. The weight % of Zn and Mg was found to decrease from top to bottom layer of the joint. The top layer showed significantly (29 %) higher weight % of Mg and Zn than other layers of the joints. The total weight % of Zn plus Mg was about 7.78 and 6.03% for top and bottom layer of the joint respectively. A Zn and Mg depletion zone can be seen (Fig. 7. a-c) irrespective of thickness for the FSW joint. Moreover, the location of Zn and Mg depletion zone was found in accordance with the failure location of the joints.

3.3 Tensile Properties

Tensile properties of the different layers of FSW joints are shown in fig. 8, found to vary through the thickness of the FSW joint. Top layer showed better combination of tensile properties than the middle and bottom layer of the joints (Refer table 3).

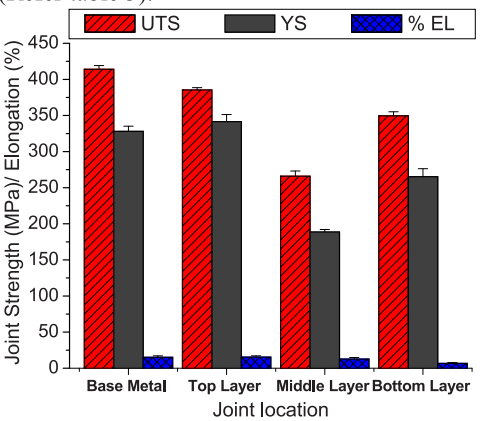

Fig. 8. Variation of tensile properties across the thickness of FSW joint

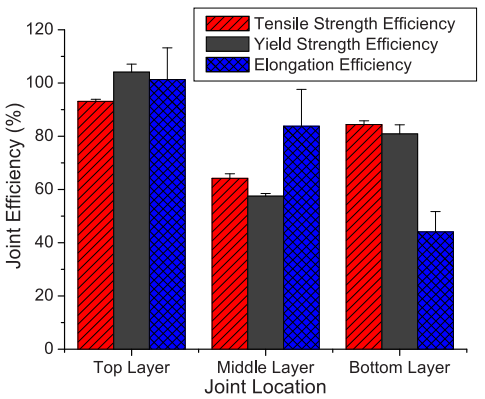

Fig. 9. Variation of joint efficiencies across the thickness of FSW joint

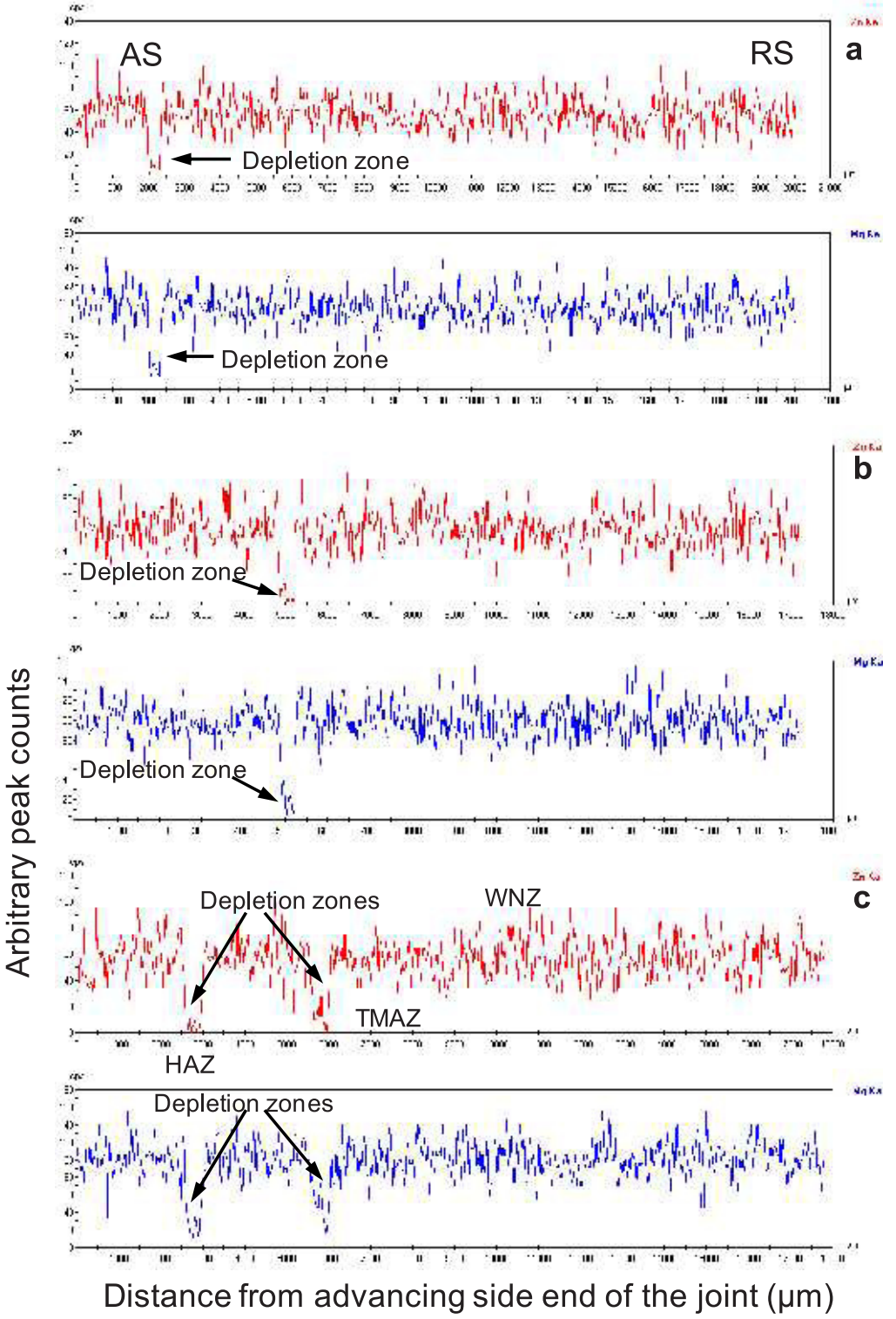

Fig. 7. Variation of Zn and Mg across transverse cross section of FSW joint (a) top, (b) middle, and (c) bottom layer

The maximum values of ultimate tensile strength (UTS), yield strength (YS) and % elongation (%EL) were 385.4 MPa, 341.5 MPa and 15.3 % respectively. On the other hand minimum values of ultimate tensile strength, yield strength and % elongation were 266.1 MPa, 188.7 MPa and 12.7 % respectively and exhibited by middle layer of the joint. The top layer exhibited slightly higher yield strength and % elongation and lower ultimate tensile strength than the base metal. Moreover, middle and bottom layers of the joints exhibited tensile properties lower than the base metal. The joint efficiency is defined as the ratio of tensile property of weld joint to that of base metal. Fig. 9 shows the variation in different joint efficiencies of different layers of the FSW joint. The top layer showed maximum tensile strength (93.1%), yield strength (104.1%) and elongation efficiency (101.3%) than middle and bottom layers of the joint. These results are in agreement with microhardness results. Liu [13] and Xu et al. [15] reported similar trend of results of tensile properties for different layers of FSW joints of AA1050-H24 and AA2219-O respectively. Tensile specimen obtained from top layer fractured from TMAZ/HAZ interface while those obtained from middle and bottom layer fractured from lower hardness region of HAZ on AS (Fig. 10). The fracture locations are in good agreement to our previous findings [16, 19].

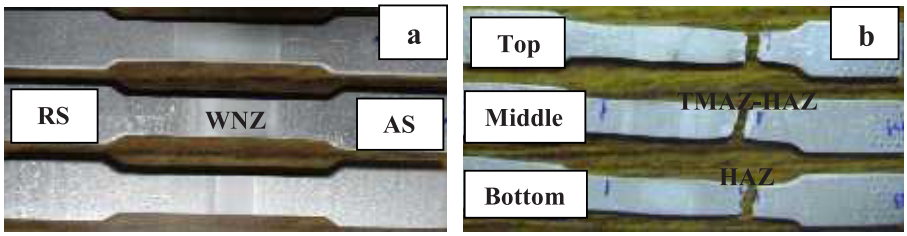

Fig. 10. Transverse tensile specimen of FSW joints (a) before, and (b) after tensile test

3.4 Fracture surfaces

Fractographs of fracture surfaces of tensile specimen obtained from top, middle and bottom layer of weld joints are shown in fig.11. No necking was observed in case of bottom layer while top layer underwent considerable necking. Top layer exhibited fracture surface covered with numerous conical depressions i.e. dimples of varying size and shapes with fractured secondary strengthening precipitates in abundant (Fig. 11. a). The mode of fracture was ductile for top layer of the joints. The strengthening precipitates rich in Zn and Mg were hard and brittle. During tensile testing these precipitates failed to maintain compatibility with the tensile deformation and get fractured thus initiated the void formation i.e. triggered the failure of the joint. Fracture was relatively less ductile for middle layer than the top layer which exhibited relatively fine dimples in less numbers along with featureless regions (Fig. 11. c). Moreover, few fractured strengthening precipitates can be seen whose EDAX analysis (Fig. 11. b) confirmed that they are rich in Zn. Fracture surface of bottom layer showed mix mode of fracture as evident from the presence featureless flat fracture surface along with fine dimples randomly distributed over the surface (Fig. 11. d). This may be due to failure of joint just after the initiation of voids. Moreover, feather marking and features that resemble cleavage facets (not shown) were also observed for bottom layer. These results are in agreement with the results of tensile test of FSW joints.

4. Discussion

FSW joints showed significant heterogeneity in respect of microstructure and mechanical properties through the thickness of the joints primarily due to development of gradient in temperature distribution and plastic strain induced during FSW. Top layer of joint which is in contact with shoulder of tool is subjected to more intensive plastic deformation and frictional heating than middle and bottom layer [5, 8 and 9]. This differential plastic deformation (and heat associated with it) and frictional heat generation establishes a temperature gradient from top to bottom. Heat from bottom layers is lost to the backing plate and fixture rapidly which in turn lowers the maximum WNZ temperature and its duration.

To understand variation in structure and mechanical properties through the thickness of weld, it is important to consider effects of severe plastic deformation and heat generation separately. Intense plastic deformation of material due to stirring action of tool during welding leads to fracture of micro-constituents and so refinement of grain structure besides work hardening and both these factors are expected to enhance hardness, and tensile properties. However, heat generation (due to friction and deformation) affecting maximum temperature and its retention time of a location can influence weld properties in three ways a) reversion of precipitates coupled with grain growth, b) reducing effect of work hardening imparted due to plastic deformation and c) reducing the flow stresses owing to temperature rise i.e. thermal softening.

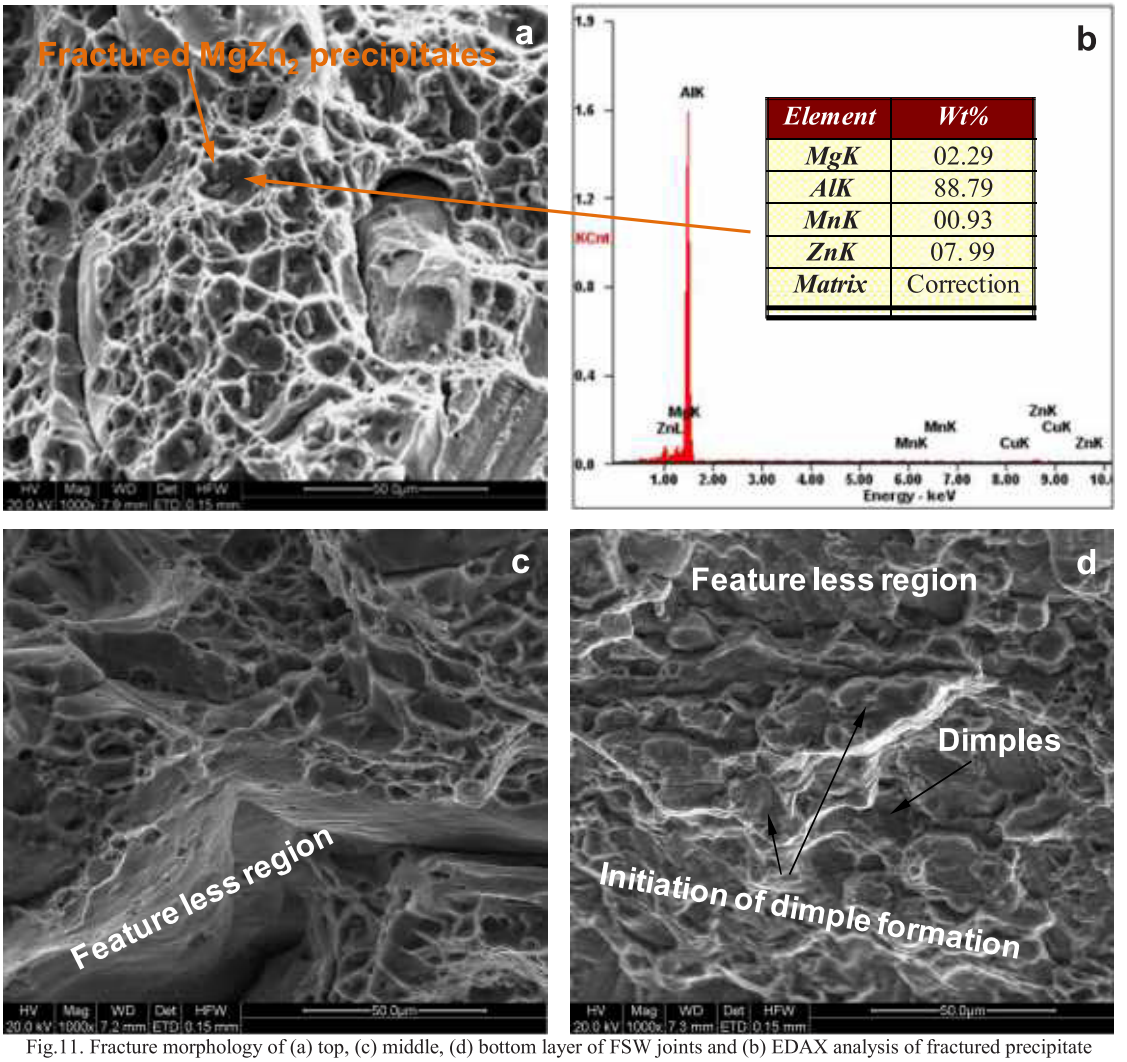

Fig.11. Fracture morphology of (a) top, (c) middle, (d) bottom layer of FSW joints and (b) EDAX analysis of fractured precipitate

Reversion followed by natural age hardening in Al-Zn-Mg alloy system increases hardness and tensile properties while grain coarsening weakens the joints. Improvement in flow of metal (due to reduction in flow stresses) is expected to enhance mechanical performance. Since flow stress decreases with increase in temperature therefore softened materials are consolidated in better way at top than in middle and bottom layer during FSW. This consolidation at high temperature helps in developing stronger joints owing to better metallurgical bonding.

Dynamic recrystallization develops fine equiaxed α aluminium grains in the central WNZ owing to higher frictional heating and plastic deformation [2, 5, 7]. Later on these grains grow statically due to effect of remaining thermal cycle of the FSW process [20-23]. High temperature of WNZ for longer time causes more static grain growth in WNZ and coarsening in HAZ in top layer of joint than bottom and middle layers which in turn leads to variation in α aluminium grains size from top to bottom. Top layer exhibited coarser α aluminium grains in the WNZ than bottom and middle layers and reversed trend was observed for TMAZ and HAZ. These finding are in good agreement to the previously reported results [7, 13, and 15]. Higher microhardness in WNZ of top layer can be attributed to solid solution strengthening and subsequent re-precipitation of fine strengthening precipitates ($MgZn_2$) owing to increased natural post weld aging response as observed maximum weld temperature are sufficiently higher than solutionizing temperature. In case of bottom layer of joint, solutionizing is incomplete and so weaker natural aging results in lower microhardness in WNZ than top layers. Higher microhardness in HAZ of bottom layer may be attributed to insignificant reversion and over aging as evident from α aluminium grains size which is nearly equal to base metal. Lowest microhardness of middle layer may be attributed to severe dissolution/coarsening of strengthening precipitates owing to retention of higher temperature for longer time than bottom layer. The microhardness results are in good agreement with the variation of weight % of Zn and Mg across the thickness of the joints. Higher weight % of Mg and Zn indicates higher density of strengthening $MgZn_2$ precipitates owing to better post weld natural aging response. Fratini et al. [24] reported increased tensile properties of water cooled friction stir weld joints of AA7075 alloy and attributed same to higher number of strengthening precipitates owing to greater number of Mg atom.

5. **Conclusion**

The influence of structural heterogeneity on mechanical properties of friction stir weld joints of AA7039-T6 alloy was investigated and following conclusion can be drawn from the result of experimental work. Microstructural heterogeneity influenced the mechanical properties of FSW joints. WNZ showed equiaxed recrystallized α Al grains finer than the base metal and size of α aluminium grains decreased from top to bottom. Mechanical properties of top layer were found superior than other layers. Top layer showed higher weight % of Zn and Mg than other layers. Top layer of the joint showed maximum microhardness in the WNZ and minimum microhardness in the HAZ. HAZ microhardness was found to increase from top to bottom. Fracture mode was ductile for top layer and whole joint while bottom surface exhibits mixed mode of fracture.

References

1. Mishra, R., S., Ma, Z.,Y., 2005. Friction stir welding and processing. Material science engineering R 50, 1–78.
2. Rhodes, C., G., Mahoney, M., W., Bingel W., H., 1997. Effects of FSW on microstructure of 7075 Al. Scripta Materilia 36, 69–75.
3. Guerra, M., Schmidt, C., McClure, J., C., Murr, L., E., and Nunes, A., C., 2003. Flow patterns during friction stir welding. Materials Characterization 49, 95–101.
4. Colligan, K., 1999. Material flow behaviour during friction welding of aluminium. Welding Journal. 229s-237s.
5. Mahoney, M., W., Rhodes, C., G., Flintoff, J., G., Spurling, R., A., Bingel, W., H., 1998. Properties of friction stir welded 7075 T651 Al, Metallurgical & Materials Transaction A 29, 1955-1964.
6. Frigaard, Ø., Grong, Ø., and Midling, O., T., 2001. A process model for friction stir welding of age hardening aluminum alloys. Metallurgical and materials transactions A 32, 1189-1200.
7. Hassan Kh., A., A., Norman, A., F., Price, D., A., and Prangnell, P., B., 2003. Stability of nugget zone grain structures in high strength Al-alloy friction stir welds during solution treatment, Acta Materialia 51, 1923-1936.
8. Chao, Y., J., Qi, X., and Tang, W., 2003. Heat transfer in friction stir welding experimental and numerical studies. Transactions of ASME 125, 138-145.
9. Zhang, Z., and Zhang, H., W., 2009. Numerical studies on the effect of transverse speed in friction stir welding. Materials and Design 30, 900-907.
10. Aval, J., C., Serjzadeh, S., and Kokabi, A., H., 2011. Theoretical and experimental investigation into friction stir welding of AA5086. International Journal of Advance Manufacturing and Technology 52, 531-544.
11. Genevois, C., Deschampa, A., and Vacher, P., 2006. Comparative study on local and global mechanical properties of 2024 T351, 2024 T6 and 5251 O friction stir welds. Material Science and Engineering A 415, 162-170.
12. Cabibbo M., McQueen, H., J., Evangelista, E., Spigarelli, S., Di Paola, M., and Falchero, A., 2007. Microstructure and mechanical property studies of AA6056 of friction stir welded plate. Material Science and Engineering A 460, 461, 86-94.
13. Liu, H., 2003. Heterogeneity of mechanical properties of friction stir welded joints of 1050-H24 aluminium alloy. Material Science Letter 22, 441-444.

14. Sato, Y., S., Watanabe, H., and Kokawa, H., 2007. Grain growth phenomena in friction stir welded 1100 Al during post weld heat treatment. Science and Technology of Welding and Joining 12, 318–323.
15. Xu, W., Liu, J., Luan, G., and Dong, C., 2009. Temperature evolution, microstructure and mechanical properties of friction stir welded thick 2219-O aluminum alloy joints. Materials and Design 30, 1886–1893.
16. Sharma, C., Dwivedi, D., K., Kumar, P., 2012. Effect of welding parameters on microstructure and mechanical properties of friction stir welded joints of AA7039 aluminium alloy. Materials and Design 36, 379-390.
17. ASTM E8/E8M-09. Standard test methods for tension testing of metallic materials1, Pennsylvania.
18. Attallah, M., M., Salem, H., G., 2005. Friction stir welding parameters: a tool for controlling abnormal grain growth during subsequent heat treatment. Materials Science and Engineering A 39, 51–59.
19. Sharma, C., Dwivedi, D., K., Kumar, P., 2012. Influence of in-process cooling on tensile behaviour of friction stir welded joints of AA7039. Journal of Material Science and Engineering A 556, 479–487.
20. Li, Y., Murr, L., E., and McClure, J., C., 1999. Flow visualization and residual microstructure associated with the friction-stir welding of 2024 aluminum to 6061 aluminum. Materials Science and Engineering A 271, 213–223.
21. Frigaard, Ø., Grong, Ø., Hjelen, J., Dahl, S., G., and Midling, O., T., 1999. Proceedings from the First International Friction Stir Welding Symposium, June 14–16, 1999 (Thousand Oaks, CA), P. Threadgill, Ed., TWI, Granta Park, U.K.
22. Sato, Y., S., Kokawa, H., Ikeda, K., Enomoto, M., Jogan, S., and Hashimoto T., 2001. Micro textures in the friction stir weld of an aluminium Alloy, Metallurgical and Materials Transactions A 32, 941-948.
23. Sato, Y., S., Urata, M., Kokawa, H., 2002. Parameters controlling microstructure and hardness during friction stir welding of precipitation hardenable aluminum alloy 6063. Metallurgical & Materials Transaction A 33, 625–635.
24. Fratini, L., Buffa, G., Shivpuri, R., 2010. Mechanical and metallurgical effects of in process cooling during friction stir welding of AA7075-T6 butt joints. Acta Materiallia 58, 2056-2067.